

Application of Levant's Differentiator for Velocity Estimation and Increased Z-Width in Haptic Interfaces

Vinay Chawda*

Ozkan Celik†

Marcia K. O'Malley‡

Department of Mechanical Engineering
and Materials Science
Rice University
Houston, TX 77005 USA

ABSTRACT

In this paper, we present results from implementation of Levant's differentiator for velocity estimation from optical encoder readings. Levant's differentiator is a sliding mode control theory-based real-time differentiation algorithm proposed as a velocity estimator. The application of the technique allows stable implementation of higher stiffness virtual walls as compared to using the common finite difference method (FDM) cascaded with low-pass filters for velocity estimation. A single degree-of-freedom (DOF) linear haptic device is used as a test bed and an automated virtual wall hitting task is implemented to experimentally demonstrate that it is possible to extend the impedance-width (or Z-width) of a haptic interface via Levant's differentiator.

Index Terms: H.5.2 [User Interfaces]: Haptic I/O—Haptic Displays; H.5.2 [User Interfaces]: Haptic I/O—Z-width

1 INTRODUCTION

Impedance-width (or Z-width) of a haptic display refers to the achievable range of impedances which the haptic device can stably present to the operator. Z-width is a fundamental measure of performance for haptic devices, as proposed by Colgate and Brown [3]. Various parameters affect the Z-width of a haptic display, including sampling period, inherent physical damping of the device, encoder quantization and filtering of velocity estimations based on encoder readings. Various strategies have been proposed to increase the Z-width of a haptic display, such as increasing the sampling rate [7] or using an optical encoder with finer resolution [3]. In this study, we aim to improve the accuracy of and decrease the delay inherent in real-time velocity estimations to extend the Z-width of a haptic display. Specifically, we experimentally evaluate the performance of Levant's differentiator [5], which is a sliding mode control theory-based differentiation method, in extending the Z-width of a single degree-of-freedom (DOF) haptic display, in comparison with commonly used finite difference method (FDM) with low-pass filtering.

Real-time estimation of velocity from optical encoder readings, in haptic interfaces or elsewhere, is ubiquitously handled by using the finite difference method, or equivalently the backward difference method. Velocity estimations via FDM result in extremely poor resolution, especially at increased sampling rates [1], and this issue is commonly resolved with a low-pass filter [3]. Low-pass filters, however, come with the cost of time delay introduced in velocity readings and act as another factor limiting the Z-width of haptic displays. More specifically, using a low-pass filter with low

(less than one tenth of Nyquist frequency) cutoff frequency would ensure that all noise is removed, but would introduce maximal time delay. On the other hand, using a low-pass filter with high cutoff frequency (close to Nyquist frequency) would result in minimal time delay, but noise may not be entirely removed. Therefore there is a trade-off between noise and time delay in velocity estimations via FDM+filtering methods.

The trade-off between noise introduced by FDM and time delay introduced by filtering has been explored in a number of studies in the literature. Bélanger et al. [1] presented results of all-integrator model-based Kalman filters for velocity and acceleration estimation from position encoder readings. Brown et al. [2] quantified the error in velocity estimation caused by use of both fixed-time and fixed-position algorithms employing backward difference estimators, Taylor's series expansion estimators and least-squares fit estimators. They concluded that fixed-time estimators are best suited to high velocities while fixed-position estimators are best suited to low velocities. They also indicated that for an application with a wide range of velocities to be measured, an algorithm switching between different estimator structures may be used. Janabi-Sharifi et al. [4] proposed an adaptive windowing method in which the window length of position readings to be used in velocity estimation is adjusted adaptively based on velocity. They verified adaptive windowing-based velocity estimation method's superior performance versus Kalman filtering and fixed-length filters. Additionally, adaptive windowing was implemented experimentally on a haptic pantograph and was shown to improve the Z-width.

In this study, we tested accuracy of Levant's differentiator [5] in estimating velocity from encoder readings and evaluated its capability for improving Z-width of haptic displays. We found Levant's differentiator to be an attractive alternative to other velocity estimators in haptic displays due to two desirable characteristics. First, Levant's differentiator does not introduce delay in estimations of velocity. Second, increasing sampling rates lead to increases in the accuracy of velocity estimations, in contrast to the generally employed FDM method. Therefore, use of Levant's differentiator provides an opportunity to achieve virtual walls with higher stiffness, since increasing loop rates will improve overall stability and decrease error in velocity estimations.

The paper is organized as follows. In Section 2, we present differentiation methods used in this study, the experimental setup and the experimental protocol we used to obtain the Z-width of the display by using Levant's differentiator and FDM+filter algorithms for velocity estimation. In Section 3, we present the obtained Z-width plots and discuss contributions and limitations of the study. Finally we conclude the paper in Section 4.

2 METHODS

In this section we first discuss the Finite Difference Method and Levant's differentiator, then describe the implementation on a single DOF haptic device and the experimental protocol.

*e-mail: vinay.chawda@rice.edu

†e-mail: celiko@rice.edu

‡e-mail: omalleym@rice.edu

V. Chawda and O. Celik contributed equally to this work.

2.1 Finite Difference Method

Let $x(t)$ represent a continuous position signal. When sampled with a sampling period of τ , position at time step i can be written as $x(i\tau)$ or simply x_i . Now consider that the absolute true position x_i is contaminated by additive noise e_i , giving the measured position as

$$y_i = x_i + e_i. \quad (1)$$

The noise can be due to various sources, such as quantization or analog-to-digital conversion. For optical encoders, quantization is the main source of noise while for analog sensors Gaussian noise due to interference and other sources dominates. The finite difference method calculates the derivative of the position signal by using two consecutive readings of position and time period [4], by Euler approximation

$$v_i = \frac{y_i - y_{i-1}}{\tau}. \quad (2)$$

It can be observed that decreasing sampling periods will lead to amplified noise from the equation

$$v_i = \frac{x_i - x_{i-1}}{\tau} + \frac{e_i - e_{i-1}}{\tau}. \quad (3)$$

Hence, increasing sampling rates significantly amplify the noise and quickly lead to unusable velocity estimations. Haptic interfaces, which require a minimum of 1 kHz loop rate for smooth and realistic rendering of virtual objects or surfaces [3], already are in the problematic region. It is important to point out that increased loop rates always improve feedback control stability and accuracy, unless an FDM operation is taking place for derivative estimation. Use of FDM for velocity estimation from position encoder readings (or estimation of derivative of error in PD controllers) is ubiquitous, and these estimated signals actually are used to add virtual damping to the system to improve stability. However, the fundamental noise amplification problem inherent within the FDM actually drives the system towards instability and limits the amount of virtual damping that is viable. It is reasonable to conclude that use of FDM for differentiation contradicts with overall feedback control goals, and is not scalable with increasing loop rates.

The most commonly used method for removing high frequency noise in velocity estimations induced by FDM is implementing a low-pass filter. Colgate and Brown [3] note that significant improvement in resolution of velocity estimations can be gained by simply using a first order low-pass filter, with almost no sacrifice in performance. In our study, we used 2nd order Butterworth filters with various (30 Hz, 100 Hz, 500 Hz, 1000 Hz) cutoff frequencies to remove the noise in FDM-based velocity estimations. These are well-known and commonly used filters in haptic and other feedback control systems.

2.2 Levant's Differentiator

Levant [5] proposed a robust exact differentiation technique based upon 2-sliding algorithm for signals with a given upper bound on the Lipschitz's constant of the derivative. Given an input signal $f(t)$, the Lipschitz's constant of the derivative is a constant C which satisfies

$$|\dot{f}(t_1) - \dot{f}(t_2)| \leq C|t_1 - t_2| \quad (4)$$

Let $W(C, 2)$ be the set of all input signals whose first order derivatives have Lipschitz's constant $C > 0$. Let the input signal $f(t)$ be Lebesgue-bounded signal in $W(C, 2)$ defined over $[0, \infty)$. It is assumed that the signals are composed of a base signal and some noise not exceeding $\varepsilon > 0$ in absolute value for a sufficiently small ε . If the second derivative of the base signal exists, then the Lipschitz's constant in equation (4) satisfies

$$\sup_{t \geq t_0} \left| \frac{d^2}{dt^2} f(t) \right| \leq C \quad (5)$$

where t_0 is the initial time.

In order to differentiate the unknown base signal, consider the auxiliary equation

$$\dot{x} = u \quad (6)$$

In the following equations, it is assumed that f, x, u_1 are measured at discrete times with time interval τ and let t_i, t, t_{i+1} be successive measuring times with $t \in [t_i, t_{i+1}]$. Define $e(t) = x(t) - f(t)$ and in order to have u as the derivative of the input signal $f(t)$, following 2-sliding algorithm is applied to keep $e = 0$

$$u = u_1(t_i) - \lambda |e(t_i)|^{1/2} \text{sign}(e(t_i)) \quad (7)$$

$$\dot{u}_1 = -\alpha \text{sign}(e(t_i)) \quad (8)$$

Here $u(t)$ is the output of the differentiator and solutions of the system described by equations (6), (7) and (8) are understood in the sense of Filippov. λ and α are strictly positive constants which determine the differentiation accuracy and must be chosen properly to ensure convergence. Levant proposed a *sufficient* condition for the convergence of $u(t)$ to $\dot{f}(t)$ given as

$$\alpha > C, \lambda^2 \geq 4C \frac{\alpha + C}{\alpha - C} \quad (9)$$

An easier choice of the parameters given in the same reference is

$$\alpha = 1.1C, \lambda = C^{1/2} \quad (10)$$

It should be noted that conditions (9) and (10) result from a very crude estimation.

One significant advantage of Levant's differentiator over FDM is that the error in derivative estimation decreases as sampling rate increases. This makes Levant's differentiator a much more desirable differentiation method for high loop rates (> 10 kHz) and a method in agreement with overall feedback control goals. Control systems employing Levant's differentiator are scalable to higher loop rates, with ever-increasing control stability and performance. On the other hand, its disadvantages are need for proper tuning of α and λ gains for differentiator convergence, need for hardware capable of high loop rates to be able to exploit its benefits (> 10 kHz) and chatter at the loop rate. This chatter is due to the switching nature of sliding mode control, and Levant [5] proposed use of low-pass filters to remove this chatter. In our paper, we opted not to use any filtering for Levant's differentiator since we wanted to evaluate the potential of it in increasing Z-width of haptic displays as a velocity estimation method under virtually no delay condition.

Figure 1 compares the derivative estimation by Levant's differentiator with adjusted gains and FDM+filter with 100 Hz cutoff frequency for a simulated damped sinusoid input signal given by

$$f(t) = 50 * e^{-t} \sin(2\pi t) \quad (11)$$

Analytical derivative is also plotted for reference. There is a reaching phase for both algorithms due to mismatch in the initial conditions, and this is more prominent for the Levant's differentiator. FDM+filter catches up in a few sampling periods but Levant's differentiator takes longer to catch up. It can be observed that derivative estimated by FDM+filter has a time-lag induced by the filter and the one estimated by Levant's method has chatter due to the switching characteristic inherent of the sliding mode control, but is virtually delay-free.

Figure 2 shows the effect of sampling frequency on the differentiation accuracy for FDM, FDM+filter, Levant's differentiator with Levant's proposed gains given by (10) and Levant's differentiator with gains tuned by manual adjustment. The input signal (11) is simulated for 5 seconds with a quantization of 1×10^{-3} to resemble a typical position encoder signal from a wall hit task. Differentiation accuracy is quantified by calculating RMS error between

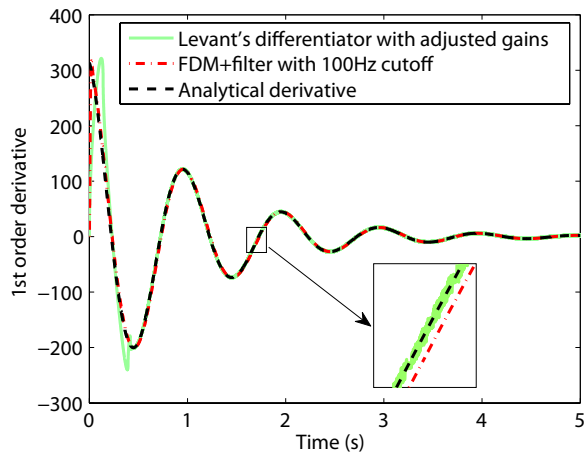


Figure 1: Comparison of the of the derivative estimated using Levant's differentiator with adjusted gains and FDM+filter with 100 Hz cutoff for a damped sinusoid signal. The inset plot shows the time-lag induced by the filter and chatter induced by Levant's method.

the derivative estimated by various differentiation schemes and the exact derivative, after allowing for a 1 second transient period for Levant's differentiators. Choosing RMS error as the error metric effectively penalizes the delay in the estimation observed with FDM+filter, as well as the high frequency chatter observed with FDM and Levant's differentiator. It is observed that the RMS error for the Levant's differentiator is higher than FDM and FDM+filter for low sampling frequencies, but as the sampling frequency increases, RMS error for the FDM and FDM+filter become increasingly larger than Levant's differentiator. The transition occurs at 10 kHz sampling frequency, where RMS error with FDM+filter is almost equal to that of the Levant's differentiator with proposed gains and the Levant's differentiator with adjusted gains performs slightly better than both. Although theoretically we expect the error for Levant's differentiator to go down with increasing sampling frequency, we observe a slight increase in RMS error after an initial drop because even though the error magnitude is going down, the switching frequency is going up, leading to an increase in RMS error.

2.3 Experimental Setup

The experimental setup consists of a one degree-of-freedom custom built impedance type haptic device that displays forces on a palm grip handle, as shown in Figure 3. A cable and pulley system connected to a permanent magnet DC motor (Faulhaber, 3557K024C) drives the handle assembly which translates on a ball-slider (Del-Tron Precision Inc., model S2-6). The motor is driven via a pulse width modulation (PWM) amplifier (Advanced Motion Controls) in current mode. A micrometer precision position encoder (Renishaw, RGH24X) is mounted on the handle assembly to accurately measure the handle position. The haptic interface has a workspace of approximately 0.15 m and a maximum continuous force output of 4 N. The bandwidth of the device is determined to be 30 Hz.

Control of the haptic device was implemented in SIMULINK and QUARC on a host computer running Windows. The code is compiled and downloaded on a target computer running QNX real-time operating system, which is interfaced to the haptic device through a Q4 data acquisition board from Quanser Inc. The sampling (and loop) rate was 10 kHz and the haptic environment was rendered at 1 kHz. More specifically, all velocity estimation algorithms in this study ran at the 10 kHz loop rate, however the actuation rate was intentionally limited by 1 kHz. This was done mainly to prevent

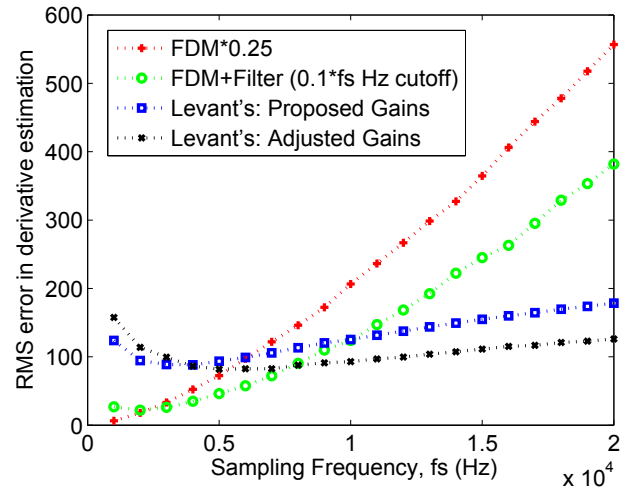


Figure 2: Plot of RMS error in derivative estimation vs. sampling frequency for various differentiation schemes. RMS error is between derivative estimated by various differentiation schemes and exact derivative after allowing for a transient time of 1s.

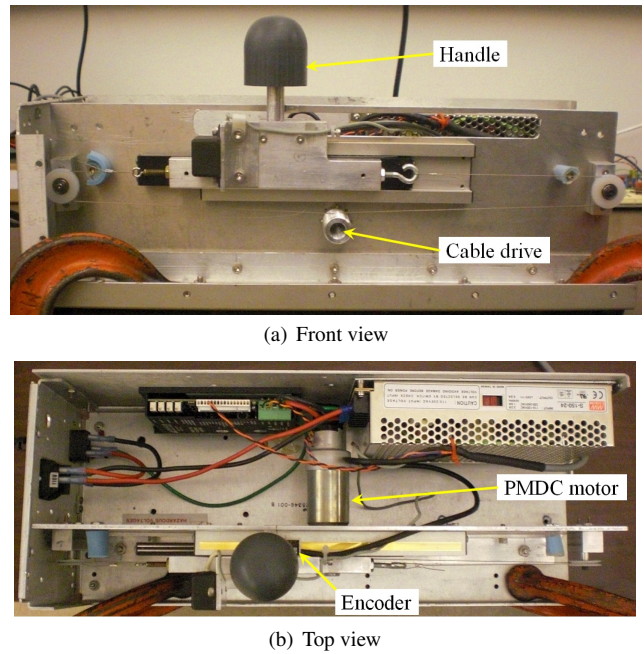


Figure 3: A single degree-of-freedom haptic device is used as the experimental setup.

the motor from hitting its current limits (or saturation) during automated wall hitting trials.

2.4 Experimental Protocol

The virtual environment implemented is a traditional virtual wall consisting of a virtual spring and a virtual damper connected in parallel with a unilateral constraint. The resulting force display is given by:

$$F = \begin{cases} K(x(t) - x_{wall}) + B\dot{x}(t), & \text{if } x(t) > x_{wall} \\ 0, & \text{if } x \leq x_{wall} \end{cases} \quad (12)$$

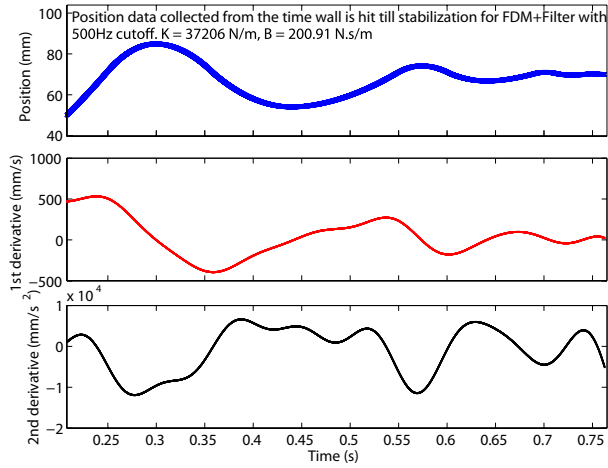


Figure 4: Estimation of the Lipschitz's constant for choosing Levant's proposed gains. The top plot is the fitted position and middle and bottom plots are the 1st and 2nd order analytical derivatives of the fitted position respectively. Supremum of the absolute value of second derivative is taken as the Lipschitz's constant.

where K is the virtual wall stiffness, B is the virtual wall damping, x_{wall} is the location of the wall and $x(t)$ is the position of the handle at any time instant t .

The selection of a spring-damper virtual wall as the haptic environment easily lends itself to using Z-width plots for classifying the impedance range of the haptic display. K and B can be set in the software, and thus the boundary between stable and unstable wall interaction can be plotted with virtual damping and virtual stiffness as the axes. The sizes of the stable regions are compared for different differentiation schemes. For creating these plots, various virtual wall interactions must be classified as stable or unstable. The presence of uncontrolled, high-frequency oscillations due to limit cycles at the wall boundary is considered as the measure for determining stability of the virtual wall hit.

At the beginning of the experiment the handle is at the home position, which is 7 cm away from and on the left side of the virtual wall. A constant force of 0.3572 N is applied by the motor which drives the handle into the virtual wall. After waiting for 4 seconds to allow the device to reach steady state, mean position is recorded. For the next 2 seconds Root Mean Square (RMS) difference between the recorded mean position and the instantaneous position of the handle is calculated. The wall hit is registered as stable if the RMS difference is below a specified stability threshold, which was set at 1.06×10^{-4} mm. Although the specific value for the threshold was chosen in an ad hoc fashion, using the same value for all experiments provided a means for fair comparison for various velocity estimation methods considered in this study.

We followed an automated experimental protocol similar to that of Mehling et al. [6], where they evaluated the effect of electrical damping in increasing Z-width of a single DOF haptic display. Our experiment begins with nominal initial stiffness and a low damping value pair (K, B) for which the hit is stable. The range of K and B values to be tested is discretized such that one step in K equals 1488.24 N/m and a step in B is 14.88 N.s/m. Stability of the wall hit for various (K, B) values is tested in an automated fashion by incrementing K in unit steps for a particular value of B until the system goes unstable. Then B is incremented by one step and if the wall hit is still unstable, K is decremented until a stable wall hit is achieved; and if the wall hit is stable then K is incremented until the wall hit goes unstable. Either way, once the stability boundary is reached, B is incremented and the cycle is repeated. (K, B) values are recorded

for all marginally unstable cases. The experiment terminates when K decreases to zero, which is the case when B is so high that the wall is unstable due to errors in velocity estimation and cannot be made stable for any value of K . The plot of (K, B) values recorded for the marginally unstable cases corresponds to the Z-width of the device. For evaluating velocity estimation algorithms' effect on the Z-width of the haptic display, the Z-width plot is generated for the following six velocity estimation methods:

1. FDM cascaded with a second order Butterworth filter with 30 Hz cutoff.
2. FDM cascaded with a second order Butterworth filter with 100 Hz cutoff.
3. FDM cascaded with a second order Butterworth filter with 500 Hz cutoff.
4. FDM cascaded with a second order Butterworth filter with 1000 Hz cutoff.
5. Levant's differentiator with the proposed gains given by equation (10).
6. Levant's differentiator with the adjusted gains, found experimentally. The gains selected are $\alpha = 1.3 \times 10^4 \text{ mm/s}^2$ and $\lambda = 50 \text{ mm}^{1/2}/\text{s}$.

The video supplement shows the stable and unstable wall hit trials with some of these velocity estimation methods. For selecting the gains α and λ proposed by Levant using equation (10), an estimate of upper bound of C is required. For this purpose, the wall hitting task was performed with velocity estimated by FDM and passed through a second order Butterworth filter with 500 Hz cutoff frequency. Position data during the hit was recorded and fitted with a sum of seven sines using the Curve Fitting Toolbox of MATLAB. Analytical double derivative of the fitted curve was calculated and its maximum absolute value attained during the hit was chosen as the estimate for C . The plots of the fitted position and its analytical first and second order derivatives are shown in Figure 4. The value of C is estimated to be $1.2 \times 10^4 \text{ mm/s}^2$, which gives the Levant's proposed gains as $\alpha = 1.32 \times 10^4 \text{ mm/s}^2$ and $\lambda = 109.54 \text{ mm}^{1/2}/\text{s}$.

3 RESULTS AND DISCUSSION

Z-width plots generated for the single DOF haptic device with derivative estimated using the six schemes listed in Section 2.4 are presented in Figure 5. The FDM+filtering method with 30 Hz cutoff frequency resulted in the smallest Z-width region among all velocity estimation methods. Increasing the filter cutoff frequency first to 100 Hz and then to 500 Hz and 1000 Hz increased the stable region significantly. Further testing using filters with cutoff frequencies up to 4000 Hz did not result in any discernible Z-width increase beyond the results obtained by using the filter with 1000 Hz cutoff. Accordingly, these results are not included here. For the FDM+filtering method with 500 Hz and 1000 Hz cutoff, the achievable stiffness values first increase and then decrease with increasing damping values, in agreement with the results in the literature [3,6]. This trend is not visible for the 30 Hz cutoff frequency case and only partially visible for the 100 Hz cutoff frequency case, due to considered range and resolution in damping on the lower end of the plot. The achievable stiffness decreases at both ends of the plot, but due to different effects. For low damping values, the amplitude of the limit-cycle-induced high frequency oscillations are large, even for small K values. For high damping values, the main problem is the delay introduced by filtering. This delay actively contributes to the generation of the limit cycles. On the other hand, the boundary of the Z-width when using Levant's differentiator is prescribed by fundamentally different factors, as discussed below.

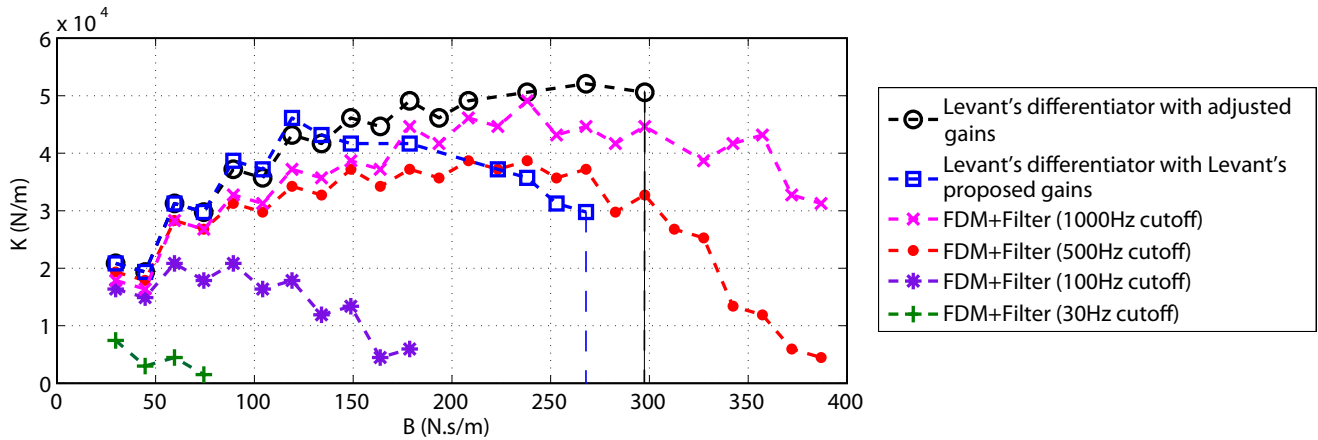


Figure 5: Z-width of the single DOF haptic device obtained with various differentiation schemes during automated wall-hitting trials.

It is observed in Figure 5 that use of Levant's differentiator for velocity estimation extends the Z-width of the device, as compared to using FDM+filter for the same purpose. Levant's differentiator with proposed choice of gains performs better than FDM+filter for damping values up to 150 N.s/m, but is found to be conservative. We adjusted the gains experimentally, thereby further increasing the Z-width of the device. Note that the adjusted gains still satisfy the sufficient condition for convergence as given by the equation (9). This behavior is in agreement with the differentiation accuracy of various differentiation methods observed at 10 kHz as shown in Fig. 2. Hence, it was possible to render higher stiffness walls stably by using Levant's differentiator in comparison with all four FDM+filter methods considered in this study, over an equal range of damping values, namely 30 N.s/m to 300 N.s/m. FDM+filter with a 500 Hz cutoff allowed stable rendering of walls with higher damping values (> 300 N.s/m) but with lower stiffness than those were possible with Levant's differentiator at lower damping values. Unlike the Z-width plots for FDM+filter methods, when Levant's differentiator is used, the stable region ends with a sharp drop at a specific damping value. This value is around 270 N.s/m for Levant's differentiator with Levant's proposed gains and it is around 300 N.s/m for Levant's differentiator with adjusted gains. The reason for this sharp drop is as K and B increases, the gains selected for the nominal case by estimating C or the ones found experimentally are no longer proper. This causes significant increase in chatter at the equilibrium position resulting in high RMS error and causing an unstable hit. A different choice of gains can extend the Z-width to higher B values but may lose stability in the lower range.

One limitation of our study is the fact that we have not handled all possible cutoff frequencies for the FDM+filter algorithm. Even when automated, generation of a Z-width map for a haptic display employing certain parameters and methods is a lengthy procedure. A more suitable way would be developing a model that would account for the limit cycles causing the high frequency noise after wall-hitting. Once such a model is developed, checking the stability and generating the Z-width maps for FDM cascaded low-pass filters with arbitrary cutoff frequency values would be much faster via simulation. It may then be possible to find the best cut-off frequency for largest Z-width via numerical optimization.

Similarly, another limitation of the study is that an exhaustive search is not conducted for the gain combination for Levant's differentiator, again to optimize Z-width by improving accuracy of velocity estimations. The convergence of the algorithm depends on the gains selected and Lipschitz's constant of the first derivative of the position signal. Therefore, although a single set of gains satis-

fying the sufficient condition (9) can guarantee convergence for a wide range of velocities, minimizing error in estimations would require online adaptation of the gains based on either the Lipschitz's constant of the velocity signal or other parameters regarding the position or velocity signal. Adaptive gain algorithms for Levant's differentiator constitutes a direction for future research.

Nevertheless, this study reports successful results from implementation of Levant's differentiator for velocity estimation and wall damping in a haptic device for the first time. The delay that is variable based on the input signal frequency content (due to the phase characteristics of the filter) is inevitable for low-pass filters and is an undesired artifact. These delays constitute the limiting factor for the Z-width at the high end of wall damping. Levant's differentiator is an attractive algorithm since its estimation errors scale down with increasing sampling rate, and with properly tuned gains, it may be possible to use it for virtually noise and delay-free velocity estimations. We believe that Levant's differentiator poses significant potential for improving derivative estimations in haptic interfaces as well as other feedback control systems.

4 CONCLUSION

In this paper, we presented an experimental implementation of Levant's differentiator algorithm as a velocity estimator from optical encoder position readings in a single DOF haptic device. By using Levant's differentiator, it was possible to increase the Z-width of the haptic display as compared to the FDM+filtering method. Levant's differentiator has the desirable characteristic that estimation errors scale down with increasing loop rates. This places it into a position where increasing loop rate improves all aspects of feedback control, without leading to a trade-off as is the case for FDM. The challenge though lies in proper tuning of the differentiator gains and need for hardware capable of high (> 10 kHz) loop rates. We proposed potential directions for future research on further improving applicability and performance of Levant's differentiator.

5 ACKNOWLEDGEMENTS

This work was supported in part by NSF Grant IIS-0812569. Authors gratefully acknowledge the assistance of J. S. Mehling in design of the experimental protocol.

REFERENCES

- [1] P. R. Bélanger, P. Dobrovolny, A. Helmy, and X. Zhang. Estimation of angular velocity and acceleration from shaft-encoder measurements. *The International Journal of Robotics Research*, 17(11):1225–1233, 1998.

- [2] R. H. Brown, S. C. Schneider, and M. G. Mulligan. Analysis of algorithms for velocity estimation from discrete position versus time data. *IEEE Transactions on Industrial Electronics*, 39(1):11–19, 2002.
- [3] J. E. Colgate and J. M. Brown. Factors affecting the z-width of a haptic display. In *Proc. IEEE International Conference on Robotics and Automation (ICRA 1994)*, pages 3205–3210. IEEE, 1994.
- [4] F. Janabi-Sharifi, V. Hayward, and C. S. J. Chen. Discrete-time adaptive windowing for velocity estimation. *IEEE Transactions on Control Systems Technology*, 8(6):1003–1009, 2002.
- [5] A. Levant. Robust exact differentiation via sliding mode technique. *Automatica*, 34(3):379–384, 1998.
- [6] J. S. Mehling, J. E. Colgate, and M. A. Peshkin. Increasing the impedance range of a haptic display by adding electrical damping. In *Proc. World Haptics Conference (WHC 2005)*, pages 257–262. IEEE, 2005.
- [7] M. K. O’Malley, K. S. Sevcik, and E. Kopp. Improved haptic fidelity via reduced sampling period with an FPGA-based real-time hardware platform. *Journal of Computing And Information Science In Engineering*, 9(1):011002–1–7, 2009.